

Estuarine Adjustment

PARKER MACCREADY

University of Washington, Seattle, Washington

(Manuscript received 18 October 2005, in final form 2 October 2006)

ABSTRACT

Subtidal adjustment of estuarine salinity and circulation to changing river flow or tidal mixing is explored using a simplified numerical model. The model employs tidally averaged, width-averaged physics, following Hansen and Rattray, extended to include 1) time dependence, 2) tidally averaged mixing parameterizations, and 3) arbitrary variation of channel depth and width. By linearizing the volume-integrated salt budget, the time-dependent system may be distilled to a first-order, forced, damped, ordinary differential equation. From this equation, analytical expressions for the adjustment time and sensitivity of the length of the salt intrusion are developed. For estuaries in which the up-estuary salt flux is dominated by vertically segregated gravitational circulation, this adjustment time is predicted to be $T_{\text{ADJ}} = (1/6)L/\bar{u}$, where L is the length of the salt intrusion and \bar{u} is the section-averaged velocity (i.e., that due to the river flow). The importance of the adjustment time becomes apparent when considering forcing time scales. Seasonal river-flow variation is much slower than typical adjustment times in systems such as the Hudson River estuary, and thus the response may be quasi steady. Spring–neap mixing variation, in contrast, has a period comparable to typical adjustment times, and so unsteady effects are more important. In this case, the stratification may change greatly while the salt intrusion is relatively unperturbed.

1. Introduction

The response of the estuarine salt intrusion to changes in river flow is of fundamental interest to both shellfish and water-quality managers, among others. A classical approach has been to develop empirical curves that relate the length of the salt intrusion L to the river volume flux Q_R (Abood 1974; Monismith et al. 2002). These curves typically result in a power law of the form $L \propto Q_R^n$. This approach appears to be justified, because the fits to data are reasonably good. Further, the specific value of n (e.g., $-1/3$) could sometimes be explained theoretically (MacCready 1999; Monismith et al. 2002; Hetland and Geyer 2004). This approach assumes a quasi-steady system, consistent with the theoretical models of Hansen and Rattray (1965) and Chatwin (1976). Kranenburg (1986) was the first to challenge the quasi-steady paradigm. He developed a theory that predicted the adjustment time T_{ADJ} for straight or widening channels and that spanned from well-mixed to partially mixed systems. His results are

mostly supported in this paper. This contribution attempts to give a clear explanation of the T_{ADJ} predictions and to explore their implications using a simple numerical model that may be readily applied to real estuaries. MacCready (1999) reviews some of the intervening developments in the understanding of estuarine adjustment, but in general little progress has been made since Kranenburg (1986). The exception is that we have a better understanding of how variations in tidal mixing interact with L (Park and Kuo 1996; MacCready 1999) and with up-estuary salt flux (Bowen 2000). Hetland and Geyer (2004) used a 3D numerical model of tidally averaged flow to test quasi-steady sensitivity of the salt intrusion to various parameters. They also explored time-dependent response and revived Kranenburg's notion that the adjustment time should vary with the freshwater filling time—a very appealing simplification that is made use of here.

2. Model development

Here a mathematical model of tidally averaged, width-averaged estuarine salinity structure in a rectangular channel of varying cross section is developed. The numerical solution to the equations is developed in this

Corresponding author address: Parker MacCready, University of Washington, Box 355351, Seattle, WA 98915-5351.
E-mail: parker@ocean.washington.edu

section, and approximate analytical solutions are developed in section 4. The model is tested against observations in section 3. The model is basically a time-dependent version of the Hansen and Rattray (1965) equations, and I attempt to make it a better predictive tool by developing parameterizations of the tidally averaged mixing coefficients. A steady version of the model was described in MacCready (2004). The approach here does not attempt to represent adequately the behavior of systems with strong lateral segregation of flow.

The state variables are $u(x, z, t)$ and $s(x, z, t)$, the tidally averaged, width-averaged velocity and salinity, where positive u and x are toward the mouth. Dividing variables into depth-mean (overbar) and deviation from depth-mean (prime) parts gives $u = \bar{u}(x, t) + u'(x, z, t)$ and $s = \bar{s}(x, t) + s'(x, z, t)$. Of these four variables, one is assumed to be known: $\bar{u} \equiv Q_R/A$, where $A(x)$ is the cross-sectional area. Then u' and s' are assumed to be in quasi-steady balance with the local along-channel salinity gradient \bar{s}_x , the mixing coefficients, and the river flow (subscripts x and t will denote partial differentiation). The quantities u' and s' have the standard cubic and quintic vertical profiles as described in MacCready (2004):

$$\begin{aligned} u' &= \bar{u}P_1 + u_E P_2 \quad \text{and} \\ s' &= (H^2/K_S)\bar{s}_x(\bar{u}P_3 + u_E P_4) \end{aligned} \quad (2.1)$$

where

$$\begin{aligned} P_1 &= \frac{1}{2} - \frac{3}{2}\zeta^2, \\ P_2 &= 1 - 9\zeta^2 - 8\zeta^3, \\ P_3 &= -\frac{7}{120} + \frac{1}{4}\zeta^2 - \frac{1}{8}\zeta^4, \quad \text{and} \\ P_4 &= -\frac{1}{12} + \frac{1}{2}\zeta^2 - \frac{3}{4}\zeta^4 - \frac{2}{5}\zeta^5. \end{aligned} \quad (2.2)$$

The magnitude of the exchange flow is $u_E = g\beta\bar{s}_x H^3 / (48K_M)$, $\zeta \equiv z/H$, and H is the channel depth. Also, K_M and K_S are the vertical eddy viscosity and diffusivity. The term $\beta \approx 7.7 \times 10^{-4} \text{ psu}^{-1}$ appears in the linearized equation of state $\rho = \rho_0(1 + \beta s)$, where ρ is the density and ρ_0 is the density of freshwater. The system thus is entirely described by the time and space evolution of the remaining state variable $\bar{s}(x, t)$, which is governed by [MacCready 2004, his Eq. (7)]:

$$\bar{s}_t + \frac{1}{A}(\bar{u}\bar{s}A)_x + \frac{1}{A}(\bar{u}'s'A)_x = \frac{1}{A}(K_H\bar{s}_x A)_x. \quad (2.3)$$

Here K_H is an along-channel eddy diffusivity due to tidal correlations of velocity, salinity, and area. Nondimensionalizing the salinity as $\Sigma \equiv \bar{s}/s_{\text{ocn}}$, where s_{ocn} is the oceanic salinity, (2.3) may be rewritten as

$$\Sigma_t = \frac{1}{A} \frac{\partial}{\partial x} \left[\underbrace{-\bar{u}\Sigma A}_{\text{River}} + \underbrace{(-\bar{u}'s'A/s_{\text{ocn}})}_{\text{Exchange}} + \underbrace{(K_H\Sigma_x A)}_{\text{Tidal}} \right], \quad (2.4)$$

where the terms on the right are associated with the three main physical mechanisms for along-channel salt transport. Using the polynomial forms for u' and s' , the “exchange” term may be expressed in terms of Σ_x , allowing (2.4) to be rewritten as

$$\begin{aligned} \Sigma_t &= \frac{1}{A} \frac{\partial}{\partial x} \{ -(\bar{u}A\Sigma) + [\bar{u}(L_{E3}^3\Sigma_x^2 + L_{E2}^2\Sigma_x + L_{E1} \\ &\quad + L_H)]A\Sigma_x \}. \end{aligned} \quad (2.5)$$

I have introduced the length scales:

$$\begin{aligned} L_{E3} &= 0.024 \left(\frac{c^4}{\bar{u}} \right)^{1/3} \frac{H^2}{(K_S K_M^2)^{1/3}}, \\ L_{E2} &= 0.031c \frac{H^2}{(K_S K_M)^{1/2}}, \\ L_{E1} &= 0.019 \bar{u}H^2/K_S, \quad \text{and} \\ L_H &= K_H/\bar{u}. \end{aligned} \quad (2.6)$$

Of the four length scales, L_{E3} is typically the most important for partially mixed systems, whereas L_H dominates in well-mixed cases. The parameter $c \equiv (g\Delta\rho H/\rho_0)^{1/2}$ is like a maximum internal wave speed, where $\Delta\rho$ is the density difference between river and ocean waters. These length scales are identical to those given in MacCready (2004) except that here K_S and K_M are allowed to vary separately.

Equation (2.5) is then solved numerically using forward time integration, with centered spatial derivatives (FTCS; Press et al. 1992). At each time step the rhs of (2.5) is evaluated and is used to advance Σ forward in time at each spatial point. At the mouth, the physical boundary condition is that the deepest salinity is equal to s_{ocn} . This may be written, using expression (2.1) for s' , as

$$\left(\frac{c^2 T_{E2}^2}{720\Delta x^2} \right) \Sigma_0^2 + \left(-\frac{2\Sigma_1 c^2 T_{E2}^2}{720\Delta x^2} + \frac{1}{15} \frac{\bar{u}T_{E1}}{\Delta x} + 1 \right) \Sigma_0 + \left(\frac{\Sigma_1^2 c^2 T_{E2}^2}{720\Delta x^2} - \frac{1}{15} \frac{\bar{u}T_{E1}}{\Delta x} \Sigma_1 - 1 \right) = 0. \quad (2.7)$$

This is a quadratic that may be solved analytically for Σ_0 . Here Σ_0 is Σ at the mouth ($x = 0$), and Σ_1 is Σ one grid point up-estuary ($x = -\Delta x$). Also $T_{E2} = H^2/(K_S K_M)^{1/2}$ and $T_{E1} = H^2/K_S$ are vertical mixing time scales that appear in (2.6). The numerical domain is made long enough that the salt intrusion never extends beyond the up-estuary limit of the grid, where $\Sigma = 0$. The grid spacing Δx is chosen so that the length of the salt intrusion is well resolved. In a typical case, $\Delta x = 1$ km is used.

The time step Δt in the FTCS scheme is changed throughout the integration to optimize the model speed while ensuring numerical stability. To do this it is noted that, neglecting the river-flow term, (2.5) may be written approximately as

$$A\Sigma_t \approx [(K_{\text{eff}})A\Sigma_x]_x, \quad (2.8)$$

where I have written the whole term in brackets in (2.5) as an effective diffusivity K_{eff} , thereby casting (2.5) as a heat equation. Then numerical stability requires (Press et al. 1992, p. 847) that

$$\Delta t \leq \frac{1}{2} \frac{\Delta x^2}{K_{\text{eff}}^{\text{max}}}, \quad (2.9)$$

where $K_{\text{eff}}^{\text{max}}$ is the maximum value of K_{eff} along the channel at the previous time step. Stable simulations are reliably achieved using Δt from (2.9) with a constant of 0.4 instead of 0.5.

3. Mixing parameterizations

The model specification is only complete when one has values for the mixing terms K_M , K_S , and K_H ; K_M and K_S are the vertical eddy viscosity and diffusivity, which relate tidally averaged turbulent fluxes to tidally averaged shear and stratification. It is assumed that they are constant over depth, but they are allowed to vary with time and along-channel distance. Parameterizations for these are sought in terms of known channel parameters (H , B , U_T) and state variables—in particular, the tidally averaged stratification Φ ; B is the channel width, U_T is the amplitude of the depth-averaged tidal velocity, and $\Phi \equiv (s_{\text{bottom}} - s_{\text{top}})/s_{\text{ocn}}$. To allow comparison with observations, H is defined as the channel *thalweg* depth and B is defined as A/H so that the cross-sectional area is correct.

A parameterization for K_M may be derived from the results of Geyer et al. (2000). They evaluated the momentum balance in the Hudson River estuary using a two-layer analytical model with no interfacial friction and found that the tidally averaged shear was approximately governed by

$$\Delta u = \frac{1}{2R} \frac{H^2 h_2}{h_1} \frac{g}{\rho_0} \frac{\partial \rho}{\partial x}, \quad (3.1)$$

where $R = 2C_{D3}U_{T3\text{rms}}$. Here Δu is the difference between outflowing and inflowing velocities averaged over upper- and lower-layer thicknesses h_1 and h_2 , $C_{D3} = 3.1 \times 10^{-3}$ is a drag coefficient referenced to 3 m above the bottom, and $U_{T3\text{rms}}$ is the root-mean-square tidal velocity at that depth. Geyer et al. (2000) discovered that the momentum balance in the lower layer was dominated by the along-channel pressure gradient and bottom friction. This sets the velocity of the inflowing deep water. They found essentially zero interfacial friction, and the velocity of the outflowing upper layer was thus set by mass conservation. Our model, which has K_M constant with depth, cannot reproduce the stress profile found by Geyer et al. (2000), because our $K_M \partial u / \partial z$ will always have nonnegligible stress at middepth. However, I can attempt to ensure that the model gives the correct relation between \bar{s}_x and the exchange flow. The cubic profile (2.1) of u has $\Delta u \equiv 1.1u_E$ (for $\bar{u} \ll u_E$). This may be combined with (3.1) from Geyer et al. (2000) (assuming $h_1 = h_2$) and solved for K_M to find

$$K_M = \frac{1.1 \times 2 \times 2}{48} HC_{D3}U_{T3\text{rms}}. \quad (3.2)$$

Then, accounting for the differences in velocity and drag coefficient of depth-averaged tidal current amplitude U_T versus the 3-m rms tidal velocity $U_{T3\text{rms}}$, the final expression for K_M is found to be

$$K_M = A_0 C_D U_T H, \quad (3.3)$$

where $A_0 = 0.065$ and $C_D = 2.6 \times 10^{-3}$. However, in the comparisons with observations (shown below) it is found that a reasonable fit required $A_0 = 0.0325$, one-half of the value derived above. The reason for the discrepancy may lie in the lateral averaging, which would require consideration of nonrectangular cross sections. This smaller value is used in all of the simulations below in which the mixing parameterizations are employed. A parameterization of the same form was used by MacCready (1999), with larger A_0 . An expression of this kind would also result from a mixing-length argument. Increasing stratification should have little effect on (3.3) because the stress is mostly in the relatively unstratified bottom boundary layer. However, note that some authors, for example Uncles and Stephens (1990), have found that the decrease of K_M by stratification is significant.

The vertical eddy diffusivity, in contrast, is focused on middepth fluxes between lower and upper layers and thus will likely be more strongly affected by stratification. Neglecting lateral variation and tidal changes

in surface height, one may define the eddy diffusivity appropriate for the tidally averaged salt balance by

$$K_S \equiv \frac{\langle \overline{\tilde{K}_S \tilde{s}_z} \rangle}{\langle \tilde{s}_z \rangle}, \quad (3.4)$$

where a tilde denotes a quantity with tidal and depth variation, an overbar is depth averaging, and angle brackets are for tidal averaging. Note that $\langle \tilde{s}_z \rangle = s'_z$ in the notation of section 2. In physical terms, K_S is the eddy diffusivity one would use with the tidally averaged stratification to achieve the tidally averaged vertical turbulent salt flux. It is assumed that the depth averaged, tidally averaged rate of loss of barotropic tidal energy goes, in part, into averaged potential energy gain due to mixing. The ratio of these is the flux Richardson number (Dyer 1997, p. 54)

$$R_f = \langle \overline{\tilde{R}_f} \rangle = \frac{-g \langle \overline{\tilde{K}_S \tilde{\rho}_z} \rangle}{\langle C_D \rho_0 \bar{u}^2 |\bar{u}|/H \rangle}, \quad (3.5)$$

where $\bar{u} = U_T \sin(\omega_T t)$. It is further assumed that this expression scales with tidally averaged properties, giving

$$R_f \propto \frac{g K_S (\rho_{\text{bottom}} - \rho_{\text{top}})}{C_D \rho_0 U_T^3}. \quad (3.6)$$

In solving for K_S , I find that

$$K_S \propto \frac{R_f C_D U_T H}{\text{Ri}_L}, \quad (3.7)$$

where Ri_L is analogous to the layer Richardson number (Lewis 1996; Dyer 1997, p. 42) but is defined with the tidally averaged stratification and by assuming that the shear scales with U_T :

$$\text{Ri}_L \equiv \frac{gH(\rho_{\text{bottom}} - \rho_{\text{top}})}{\rho_0 U_T^2} = \frac{c^2 \Phi}{U_T^2}. \quad (3.8)$$

Note that c and U_T are known environmental parameters, whereas Φ is a state variable. Expression (3.7) decreases with Ri_L , an expected result of increasing stratification; however, R_f is an unknown function of Ri_L . It is proposed that K_S may be parameterized using a function of the following form:

$$K_S = A_1 C_D U_T H \left(A_3 + \frac{1 - A_3}{1 + A_2 \text{Ri}_L} \right), \quad (3.9)$$

with A_1 , A_2 , and A_3 being empirically derived constants. The maximum value of K_S is $A_1 C_D U_T H$, much like K_M in (3.3), and so it is expected that $A_1 \leq A_0$. The rate of decrease of K_S with increasing Ri_L is governed by A_2 , analogous to the parameterization in Munk and Anderson (1948). The minimum value of K_S as $\text{Ri}_L \rightarrow \infty$ is

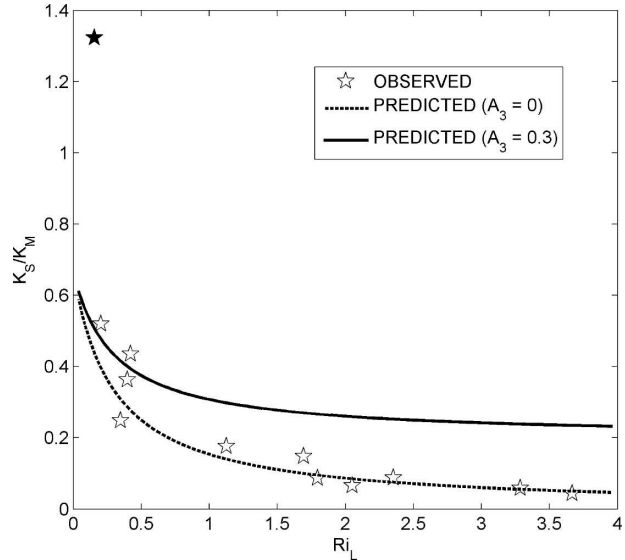


FIG. 1. The ratio of the vertical eddy diffusivity to the vertical eddy viscosity, vs the layer Richardson number, calculated from the parameterizations (3.3) and (3.9), with two values of the parameter A_3 (solid and dashed lines). The same quantity calculated from the Hudson River observations of Peters (1999) is plotted as stars. The parameterization (3.9) with $A_3 = 0$ is designed to fit the observations, except for one instance, which is highlighted as a filled star.

given by A_3 times its maximum value ($0 \leq A_3 \leq 1$); A_3 is intended to represent the potential effects of a channel with shallow sides. On the sides, the most stratified water (which is at middepth in the center of the channel) will intersect with the sloping sidewalls and will be subject to turbulence generated by the bottom boundary layer. Nonzero A_3 implies that, even with strong midchannel stratification, turbulent buoyancy flux cannot be entirely shut down on the edges.

To determine A_1 and A_2 , I will fit to inferred values of turbulent salt flux from observations made in the Hudson River estuary (Peters 1999). Because these data were generally taken in 15 m of water and not on the sidewalls, I will perform the fit by assuming $A_3 = 0$ and will then use other criteria later to estimate A_3 . Peters (1999, his Table 4) gives turbulent salt flux (inferred from dissipation) at the depth of the greatest stratification, integrated over the full tidal cycle, for 12 cases. For these he also gives U_T (his Table 2), and one may take the tidally averaged bottom-to-top salinity difference graphically from his Fig. 7. For our polynomial form of s , one may show that the peak value of $\partial s/\partial z$ is equal to $1.7(s_{\text{bottom}} - s_{\text{stop}})/H$, allowing us to express Peters's observations in terms of the variables in (3.9), with $A_3 = 0$. The results of this comparison are plotted in Fig. 1. A reasonable fit between prediction and observations is found using $A_1 = 0.022$ and $A_2 =$

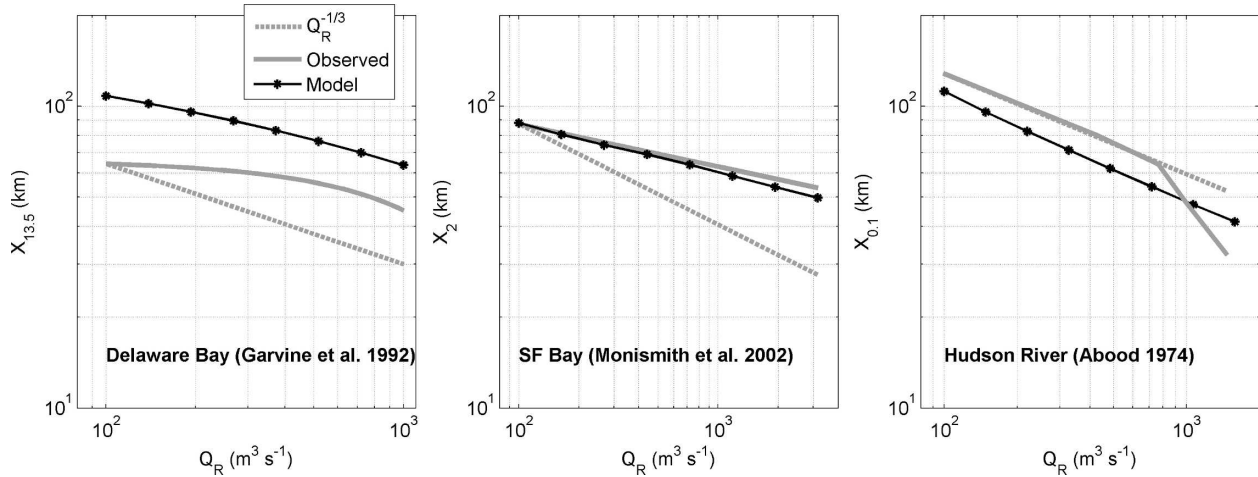


FIG. 2. Model quasi-steady salt intrusion vs Q_R , for three estuaries, as labeled. The salt intrusion is defined by a different salinity in each case: e.g., $X_{13.5}$ means the salt intrusion defined by $\bar{s} = 13.5$. Observed curves are also plotted, as is a curve proportional to $Q_R^{-1/3}$ for reference.

3.33. There is one observation, highlighted in Fig. 1, that my parameterization does not predict at all well. This occurred during spring tide, with the lowest observed tidally averaged stratification (1.5 psu). There is no obvious explanation for this discrepancy. In finishing the parameterization of K_S , it is assumed that $A_3 = 0.3$, the reasons for which are discussed at the end of this section.

The final parameterization that is required is for K_H , the along-channel mixing term. Banas et al. (2004) found a good fit for observations in Willapa Bay using $K_H = 0.035U_T B$, with the mixing being due to lateral stirring by tidal eddies in that complex, multichannel system. This parameterization is adopted here but is generalized to cases in which the tidal excursion $L_T \equiv U_T T_T / \pi$ (where T_T is the tidal period) is smaller than B and thus is the limiting factor for the stirring. Near the mouth of the estuary, along-channel flux is enhanced by efficient exchange between the mouth and the coastal ocean (Stommel and Farmer 1952). MacCready (2004) expressed this idea in terms of a K_H , which decreased from a theoretically derived maximum value near the mouth K_{HM} , to a smaller value landward. Based on 3D numerical experiments (not shown here) it is assumed that this portion of K_H near the mouth decays linearly from K_{HM} to zero over L_T , and that K_{HM} is decreased from the value derived in MacCready (2004) by a factor ε ($0 \leq \varepsilon \leq 1$) because the presence of the river plume will decrease the efficiency of estuary–ocean exchange. To summarize, in the current model I will use

$$K_H = \max \left\{ \begin{array}{l} 0.035U_T \min(B, L_T) \\ K_{HM}(1 + x/L_T) \end{array} \right. , \quad (3.10)$$

where x is the along-channel coordinate, with $x = 0$ at the mouth and negative in the up-estuary direction. The value of the diffusivity at the mouth is given by

$$K_{HM} = \varepsilon \frac{L_T U_T}{\pi} \left[1 - \left(\frac{2B}{\pi L_T} \right)^{1/2} \right]. \quad (3.11)$$

A reasonable fit to observations (below) is found with $\varepsilon = 0.1$, and thus K_{HM} is a factor-of-10 smaller than that proposed in MacCready (2004). This parameter is very poorly constrained, however, and would be a good topic for future studies.

One may test this model and its mixing parameterizations, using observations of the length of the salt intrusion L versus river flow. Doing this for Delaware Bay (Garvine et al. 1992), northern San Francisco Bay (Monismith et al. 2002) and the Hudson River (Abood 1974) gives the results plotted in Fig. 2. The model compares fairly well to San Francisco Bay and the Hudson, notably capturing the observed insensitivity of L to Q_R in the San Francisco Bay case. On the other hand, the model seriously overpredicts the length of the salt intrusion in the Delaware Bay. This is potentially because the Delaware bathymetry has a deep middle channel cut into a very wide, shallow bay, whereas our model treats the estuarine cross section as rectangular. The salt flux in the Delaware may also be more laterally segregated, whereas this model assumes it to be vertically segregated. The fit to Delaware observations was actually better in MacCready (2004); however, in that case the diffusivities were chosen to achieve the best fit instead of being given by the parameterization derived in this section. There is no obvious way to remedy this

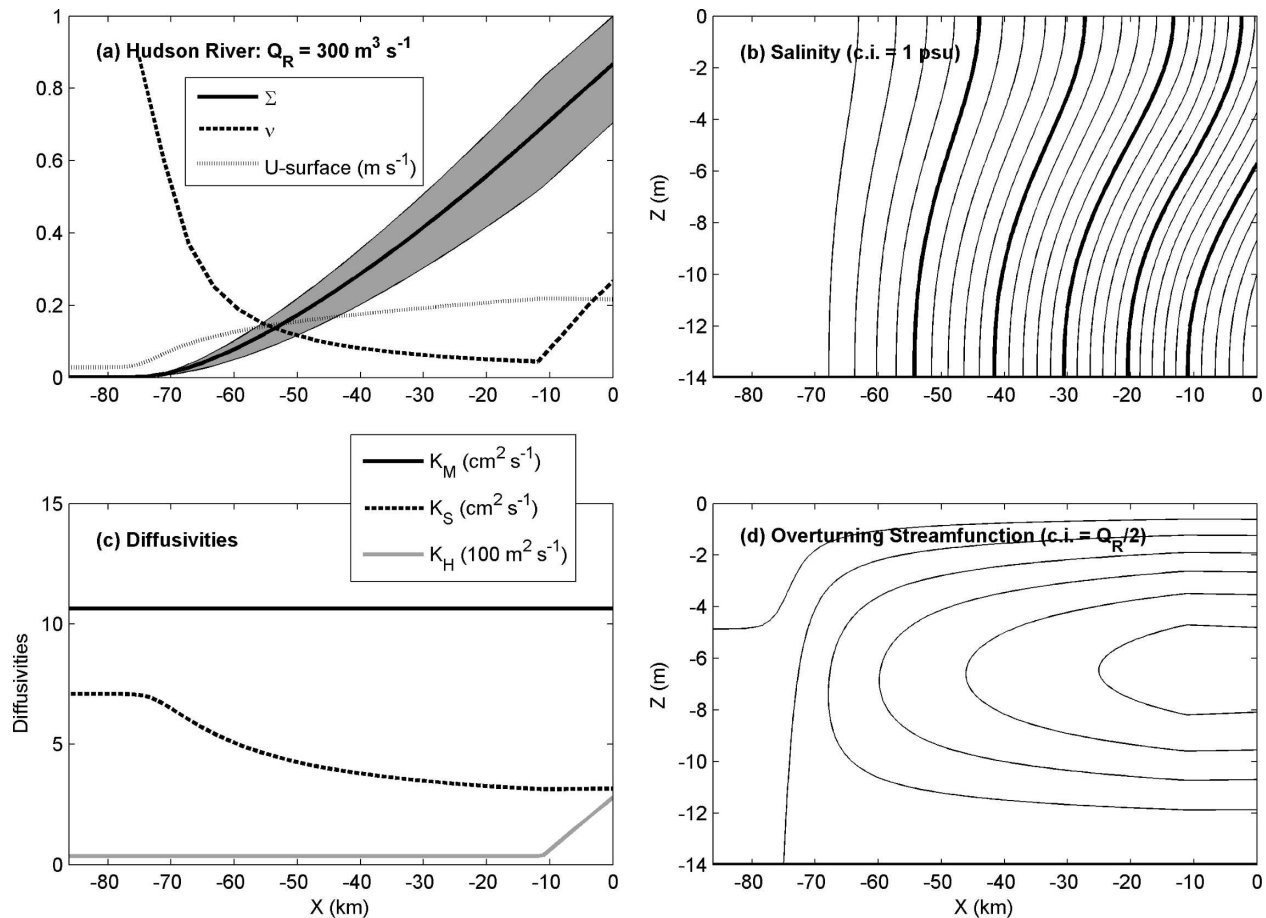


FIG. 3. Quasi-steady model solution for the Hudson River, under moderate-flow conditions and average tides. (a) The dimensionless salinity Σ vs x is plotted as a thick line, with the stratification shown as a gray band around it. The surface velocity and ν (the diffusive fraction of up-estuary salt flux) are also shown. (b) The salinity vs x and z . (c) Distributions of the parameterized diffusivities. (d) The overturning streamfunction normalized by Q_R , showing the exchange flow (the sense of the circulation is generally clockwise on the page).

short of reworking the model formulation to account for different cross-sectional shapes or salt flux mechanisms. Examples of equilibrium fields for the Hudson River solution are plotted in Fig. 3. The Hudson is modeled as a straight channel, 14 m deep, and 1.14 km wide with $Q_R = 300 \text{ m}^3 \text{ s}^{-1}$ and $U_T = 0.9 \text{ m s}^{-1}$. Northern San Francisco Bay has variable depth and width, as described in MacCready (2004), and $U_T = 0.85 \text{ m s}^{-1}$. Delaware Bay has $H = 14 \text{ m}$, and $U_T = 0.8 \text{ m s}^{-1}$. The area A is 0.32 km^2 over the 20 km nearest the mouth and decays exponentially up-estuary from that, with a length scale of 25 km, to a minimum of $A = 10^4 \text{ m}^2$. Extensive experimentation with different mixing parameterization coefficients gave rise to the values given in the text above, but one cannot be certain that these are optimum choices.

These systems span a wide range of coastal plain estuaries, from wide to shallow and from well mixed to

highly stratified, depending on Q_R . The model captures the basic response of L to Q_R in two of the three cases. The model differs from that derived in MacCready (2004) in that it incorporates time dependence and the above mixing parameterizations. I proceed, assuming that the model gives a reasonable approximation of estuarine dynamics over a wide range of forcing. The purpose of this model is to explore estuarine adjustment over a wide range of parameter space, and so its simplicity and rapid numerical integration are real benefits. Specific estuaries are best left to detailed 3D models, as epitomized by the recent work in the Hudson of Warner et al. (2005).

4. Linear adjustment time theory

Before using the model to explore responses to unsteady forcing, it is useful to develop a theoretical ex-

pectation. The derivation here is in some ways similar to that in MacCready (1999) but is substantially simplified by expressing the adjustment time in terms of the hydraulic replacement time L/\bar{u} , as suggested by Kranenburg (1986), Bowen (2000), and Hetland and Geyer (2004). It differs from Kranenburg (1986) in that the separate contributions of the exchange flow versus tidal stirring are made explicit, as are the physics of the response to different types of forcing. In addition, the consequences of the adjustment time for estuarine sensitivity are explored.

The along-channel integral of the salt balance (2.5) gives

$$\frac{d}{dt} \int_R^0 \Sigma dx = [-\bar{u}\Sigma + \bar{u}(L_{E3}\Sigma_x)^3 + \bar{u}L_H\Sigma_x]_{x=0}, \quad (4.1)$$

where $x = R$ is some position up-estuary at which $\bar{s} = 0$, and $x = 0$ at the mouth. In deriving (4.1) it has been assumed that A is equal to a constant and that the exchange flow is dominated by the L_{E3} term (Monismith et al. 2002; MacCready 2004). Next, by assuming that the salinity structure may be described very approximately as decreasing linearly from s_{ocn} to zero over the distance L , one may scale terms in (4.1) as

$$\int_R^0 \Sigma dx \propto L/2 \quad \text{and} \quad \Sigma_x \propto 1/L. \quad (4.2)$$

Substituting these into (4.1) gives

$$\frac{dL}{dt} = -2\bar{u}\Sigma|_{x=0} + 2\bar{u}\left(\frac{L_{E3}}{L}\right)^3 + 2\bar{u}\left(\frac{L_H}{L}\right); \quad (4.3)$$

thus the problem is reduced from a PDE in $\Sigma(x, t)$ to a nonlinear ODE in $L(t)$. It is also implicit in (4.3) that the values of L_{E3} and L_H at $x = 0$ are representative of their values over L . One may express L as the sum of a mean state and some variation about that state: $L(t) = L_0 + L'(t)$. Then, for small variations $|L'| \ll L_0$, one may linearize (4.3) using the leading terms in the power series expansions of L^{-3} and L^{-1} to find an equation that is linear in L' :

$$L'_t = -2\bar{u}\Sigma|_{x=0} + 2\bar{u}\frac{L_{E3}^3}{L_0^3}\left(1 - 3\frac{L'}{L_0}\right) + 2\bar{u}\frac{L_H}{L_0}\left(1 - \frac{L'}{L_0}\right). \quad (4.4)$$

This may be forced in a variety of ways, allowing river flow, tidal mixing, or even the oceanic salinity to change. These may also be written in terms of small variation about a mean value. To first order in the perturbation terms, these are

$$\text{change river flow: } \bar{u} = \bar{u}_0 + \bar{u}',$$

$$\text{change ocean salinity: } \Sigma|_{x=0} = 1 + \Sigma',$$

$$\text{change tidal mixing or river flow: } L_{E3}^3 = L_{E30}^3\left(1 - \frac{\bar{u}'}{\bar{u}_0} - 3\frac{K'_V}{K_{V0}}\right), \quad \text{and}$$

$$\text{change tidal stirring or river flow: } L_H = L_{H0}\left(1 - \frac{\bar{u}'}{\bar{u}_0} + \frac{K'_H}{K_{H0}}\right), \quad (4.5)$$

where $K_V = K_{V0} + K'_V$, [K_V is an approximation of the vertical mixing coefficients, given by $K_V = (K_S K_M^2)^{1/3}$] and $K_H = K_{H0} + K'_H$; also

$$L_{E30}^3 = \frac{(0.024)^3 c^4 H^6}{\bar{u}_0 K_{V0}^3} \quad \text{and} \quad L_{H0} = \frac{K_{H0}}{\bar{u}_0}. \quad (4.6)$$

Substituting these into (4.4) and again retaining terms only to first order, it is found (dividing by L_0) that

$$\left(\frac{L'}{L_0}\right)_t = \frac{2\bar{u}_0}{L_0} \left[-\frac{\bar{u}'}{\bar{u}_0} - \Sigma' + \frac{L_{E30}^3}{L_0^3} \left(\frac{-3K'_V}{K_{V0}} \right) + \frac{L_{H0}}{L_0} \left(\frac{K'_H}{K_{H0}} \right) \right] + \frac{2\bar{u}_0}{L_0} \left[\frac{L_{E30}^3}{L_0^3} \left(\frac{-3L'}{L_0} \right) + \frac{L_{H0}}{L_0} \left(\frac{-L'}{L_0} \right) \right]. \quad (4.7)$$

TABLE 1. Theoretical predictions for the adjustment time and sensitivity, given in dimensional format.

System type	Adjustment time: T_0/γ	Forcing (what varies)	α	γ	Sensitivity: $(\alpha/\gamma)/[1 + (\omega T_{\text{ADJ}})^2]^{1/2}$
Exchange dominated	$\frac{1}{6}(L_0/\bar{u}_0)$	River flow	-1	3	$(-1/3)/[1 + (\omega T_{\text{ADJ}})^2]^{1/2}$
		Ocean salinity	-1	3	$(-1/3)/[1 + (\omega T_{\text{ADJ}})^2]^{1/2}$
		Tidal mixing	-3	3	$(-1)/[1 + (\omega T_{\text{ADJ}})^2]^{1/2}$
Tidal stirring dominated	$\frac{1}{2}(L_0/\bar{u}_0)$	River flow	-1	1	$(-1)/[1 + (\omega T_{\text{ADJ}})^2]^{1/2}$
		Ocean salinity	-1	1	$(-1)/[1 + (\omega T_{\text{ADJ}})^2]^{1/2}$
		Tidal stirring	1	1	$(+1)/[1 + (\omega T_{\text{ADJ}})^2]^{1/2}$

In deriving (4.7) I have made use of the identity $1 = (L_{E30}/L_0)^3 + L_{H0}/L_0$, which may be shown from (4.4) by setting all primed quantities to zero. A dimensionless form of (4.7) may be derived by defining dimensionless quantities

$$\lambda \equiv \frac{L'}{L_0} \quad \text{and} \quad \tau \equiv \frac{t}{T_0}, \quad \text{where} \quad T_0 \equiv \frac{1}{2} \frac{L_0}{\bar{u}_0}. \quad (4.8)$$

The quantity T_0 is approximately the freshwater replacement time over the length of the salt intrusion. For the sake of obtaining a simple theoretical prediction it is assumed that tidal mixing is solely proportional to the amplitude of the tidal velocity, with $U_T = U_{T0} + U'_T$, so that $K'_V/K_{V0} = K'_H/K_{H0} = U'_T/U_{T0}$. Thus for the moment I am suspending the more complicated mixing parameterizations from the previous section. Under this assumption, and applying (4.8), one may write the equation for λ concisely. To allow comparison with numerical simulations (shown below) this is done in two limits. First, for exchange dominated flows ($L_{E30}^3/L_0^3 \rightarrow 1$; $L_{H0}/L_0 \rightarrow 0$) the governing equation is

$$\frac{d\lambda}{d\tau} = \left(-\frac{\bar{u}'}{\bar{u}_0} - \Sigma' - 3\frac{U'_T}{U_{T0}} \right) - 3\lambda. \quad (4.9)$$

In the tidal-stirring dominated limit ($L_{E30}^3/L_0^3 \rightarrow 0$; $L_{H0}/L_0 \rightarrow 1$) the governing equation is

$$\frac{d\lambda}{d\tau} = \left(-\frac{\bar{u}'}{\bar{u}_0} - \Sigma' + \frac{U'_T}{U_{T0}} \right) - \lambda. \quad (4.10)$$

These both have the form of a forced, damped, linear, first-order ODE, which may be written generally as

$$\frac{d\lambda}{d\tau} = \alpha F - \gamma \lambda, \quad (4.11)$$

where α and γ are numerical constants (± 1 and 3), and F is the dimensionless forcing: \bar{u}'/\bar{u}_0 , Σ' , or U'_T/U_{T0} . An equation of this form was used in Hetland and Geyer (2004) to analyze their numerical results. What has been done here is to demonstrate how such a form arises naturally from the estuarine system of equations. Monismith et al. (2002) also used an equation similar in

form to (4.11), but with a nonunity exponent on the damping term.

If (4.11) is an adequate representation of the linearized estuarine adjustment problem, it gives a number of useful results. For step changes in forcing, (4.11) predicts exponential adjustment toward a new steady state in a time

$$\tau_{\text{ADJ}} = \frac{1}{\gamma}, \quad \text{or} \quad T_{\text{ADJ}} = \frac{1}{\gamma} T_0 = \frac{1}{\gamma} \frac{1}{2} \frac{L_0}{\bar{u}_0}, \quad (4.12)$$

where both the dimensionless (τ_{ADJ}) and dimensional (T_{ADJ}) forms of the adjustment time are given. MacCready (1999) argues that a full characterization of the adjustment problem also requires that one know the sensitivity, defined as

$$\text{Sens} \equiv \frac{\text{max change in } \lambda}{\text{max change in } F}. \quad (4.13)$$

MacCready (1999) gave theoretical expressions for Sens while considering changes in a system that had fully equilibrated to a step change in forcing. However, a more important aspect of the sensitivity arises in systems with continuously varying forcing. In mathematical terms, consider the case of periodic forcing $F = F_0 \sin(\Omega\tau)$, where $\Omega = \omega T_0$ is the dimensionless forcing frequency. Then the solution to (4.11) is

$$\lambda = \frac{\alpha F_0/\gamma}{[1 + (\Omega/\gamma)^2]^{1/2}} \sin \left[\Omega\tau - \tan^{-1} \left(\frac{\Omega}{\gamma} \right) \right]. \quad (4.14)$$

A solution of similar form was given in Hetland and Geyer (2004). The term Ω/γ may also be written as ωT_{ADJ} so that it expresses the ratio of the adjustment time to the forcing period (times 2π). For very gradual forcing variation $\omega T_{\text{ADJ}} \rightarrow 0$, and so the response is quasi steady, given by $\lambda = \alpha F/\gamma$. However, as the forcing variation becomes more rapid the response of λ lags the quasi-steady response and decreases in amplitude. For (4.14), the sensitivity is

$$\text{Sens} = \frac{\alpha/\gamma}{[1 + (\Omega/\gamma)^2]^{1/2}}. \quad (4.15)$$

The theoretical results are summarized in Table 1.

There is also a more intuitive way to understand the theoretical adjustment times given in Table 1. MacCready (1999) noted that the adjustment process could be thought of in terms of an adjustment to small step changes in forcing. Then the adjustment time is given by the net change in salt of the system over the course of the adjustment, divided by the rate of addition/removal of salt at the start of the adjustment. In looking at Table 1, it is seen that the adjustment time in the exchange-dominated cases is given by $(1/6)L_0/\bar{u}_0$, both for changes in river flow and changes in tidal mixing. This seems curious, given that the two forcing processes are so different. For either process a factor of $1/2$ in the adjustment time results from the fact that the net salt in the system is proportional to one-half of the length of the salt intrusion. This leaves us to explain the remaining factor of $1/3$. For the case of changing river flow, the salt intrusion length varies as $\bar{u}^{-1/3}$; therefore, in our linearized approach the net salt will vary as $-(1/3)\bar{u}$. The initial rate of change of net salt is due to increased section-averaged advection at the mouth and so varies as $-\bar{u}$. The ratio of these is $1/3$, which is the desired result. In the case of varying tidal mixing, on the other hand, the salt intrusion length varies as K_V^{-1} , or $-K_V$ in the series expansion. The initial rate of change of net salt (after the stratification and exchange flow have adjusted to the new mixing levels, but before the length of the salt intrusion has adjusted) varies as K_V^{-3} , or $-3K_V$ in the series expansion. The ratio of these is again $1/3$, but it is clear that the physics leading to this result is very different in the two cases.

The theoretical predictions may be tested using the numerical model developed in section 2. The model is run in two limits; in both cases I do not use the mixing parameterization of section 3 and instead set the mixing coefficients by hand (all constant in x but potentially functions of time). In the exchange-dominated limit, I set $K_H = 0$, $K_M = 14 \text{ cm}^2 \text{ s}^{-1}$, and $K_S = K_M/3$. For the tidal-stirring-dominated limit, I set $K_M = K_S = 100 \text{ cm}^{-1} \text{ s}^{-1}$, effectively making the system well mixed in the vertical direction, and set $K_H = 200 \text{ m}^2 \text{ s}^{-1}$. For both cases, the estuary is 10 m deep, 1000 m wide, and 400 km long (longer than the greatest salt intrusion in all cases). Eighteen simulations in each limit were performed, using combinations with average values of river flow given by $Q_R = (50, 100, 200) \text{ m}^3 \text{ s}^{-1}$ and mixing coefficients multiplied by factors of 0.5, 1, and 2. For each of these nine combinations, either Q_R or U_T was varied periodically in time by $\pm 10\%$, with a period of 50 days. Simulations lasted four forcing periods, by which time a nearly periodic solution was obtained. The salt intrusion length L was calculated for the final forcing period as $2\int \Sigma dx$. The time averages of

L and \bar{u} were used to calculate T_0 , τ , Ω , L_0 , and λ . A least squares fit of λ to a function of the form $\lambda = C_1 \sin(\Omega\tau) + C_2 \cos(\Omega\tau)$ gives estimates for C_1 and C_2 . From these, one may make two direct comparisons between the model results and the theory, using the relations

$$T_{\text{ADJ}} = \frac{-C_2}{C_1\omega} \quad \text{and} \quad \text{Sens} = \frac{(C_1^2 + C_2^2)^{1/2}}{F_0}. \quad (4.16)$$

These are plotted in Fig. 4 for all simulations (35 out of 36) for which the calculated T_{ADJ} was less than 50 days. These spanned a range of L_0 from 7 to 158 km. Overall, there is reasonable agreement between the analytical theory and numerical model despite the many simplifying assumptions used to derive the linear equation in (4.11). Most of the model adjustment times are within a factor of 2 of the theory, with the theory always underpredicting exchange-dominated cases, as was seen also in Hetland and Geyer (2004). The magnitude of the model sensitivity is generally less than that of the theory. The model adjustment times span from 1.6 to 45 days, and the factor $(1 + \Omega^2/\gamma^2)^{-1/2}$ from Sens goes from 0.98 to 0.17. In physical terms, estuaries in which the adjustment time is comparable to the forcing period will exhibit much-decreased sensitivity. This is because the length of the salt intrusion does not have time to equilibrate with the forcing. The simulations done here range from nearly equilibrated to very nonequilibrated.

5. Consequences of unsteadiness

In running the complete model (with the full mixing parameterizations from section 3) for San Francisco Bay, Delaware Bay, and the Hudson River estuary, the adjustment times given in Table 2 are found. Adjustment times listed there are calculated using the model configurations from Fig. 2, and varying Q_R by $\pm 10\%$ about either 100 or 1000 $\text{m}^3 \text{ s}^{-1}$, with forcing periods of 50 or 100 days. The longer forcing periods are required to obtain reliable estimates for cases with longer adjustment times. Results for varying U_T were similar, although in some cases (especially Delaware Bay) no T_{ADJ} could be calculated, perhaps because of the competing tendencies of the exchange flow and tidal stirring. The adjustment times vary from T_0 to $T_0/6$, whereas the theory from section 4 implies a range from T_0 to $T_0/3$. Another trend is that all of the high-flow cases are a greater fraction of T_0 than are the low-flow cases, contrary to what one might expect given that the high-flow cases tend to be more exchange dominated. Thus, although the theory may be a reasonable guide to adjustment times, it can also be off by as much as a

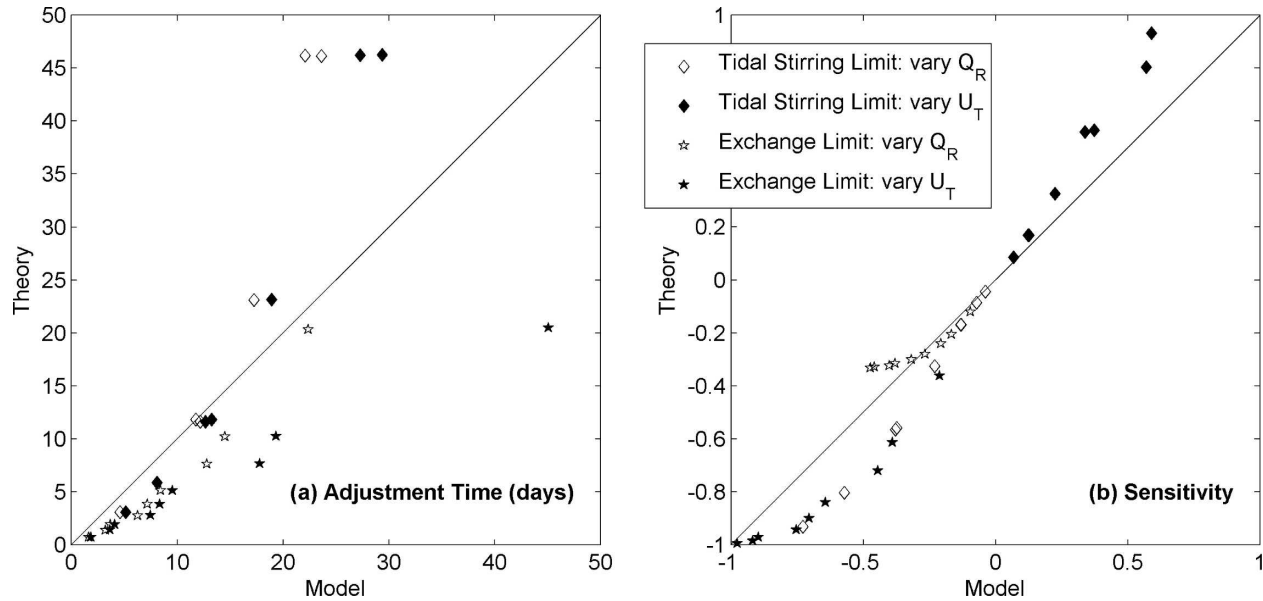


FIG. 4. (a) Adjustment times and (b) sensitivities for 35 numerical simulations. Theoretical values (from Table 1) are plotted against numerical model results. Both exchange-dominated and tidal-stirring-dominated cases are considered. In either case, the forcing is due to variation of either river flow or tidal mixing, with a period of 50 days. Cases with the longest adjustment times correspond to those with the smallest sensitivities.

factor of 3, and detailed observations and modeling are clearly required for specific estuaries. The San Francisco Bay adjustment times in Table 2 bracket the observational estimate of 12 days given in Monismith et al. (2002), although they found no significant trend of the adjustment time relative to Q_R . The long adjustment times in Delaware Bay suggest that it may be significantly out of equilibrium much of the time, similar to the results of Banas et al. (2004) for Willapa Bay.

Vertical stratification and the exchange flow are more strongly affected by changes in mixing when the length of the estuary is not in equilibrium (Park and Kuo 1996; MacCready 1999; Hetland and Geyer 2004). This may be shown from the linear theory of the previous section. For $\bar{u} \ll u_E$, the dimensionless stratification is

$$\Phi \equiv \frac{s_{\text{bot}} - s_{\text{top}}}{s_{\text{ocn}}} \approx \frac{3}{20} u_E \frac{H^2}{K_S} \Sigma_x \quad (5.1)$$

and $u_E = c^2 \Sigma_x H^2 / (48 K_M)$; therefore,

$$\Phi \approx \frac{c^2}{320} \frac{H^4}{K_S K_M L^2} \frac{1}{L^2}. \quad (5.2)$$

Expanding K_S , K_M , and L in terms of small variations about a mean value, one may express Φ to leading order as

$$\Phi \approx \frac{c^2}{320} \frac{H^4}{K_{V0}^2 L_0} \left(1 - 2 \frac{U'_T}{U_{T0}} - 2\lambda \right). \quad (5.3)$$

For the case of an exchange-dominated estuary forced by varying U_T , (4.9) becomes $\lambda_\tau = -3U'_T/U_{T0} - 3\lambda$, which may be substituted into (5.3) to give

$$\Phi \approx \frac{c^2 H^4}{320 K_{V0}^2 L_0^2} \left(1 + \frac{2}{3} \lambda_\tau \right). \quad (5.4)$$

This predicts that Φ can grow much larger or smaller than its equilibrium value when $|\lambda_\tau|$ is not small relative to 1. From (4.14) one may show that the dependence of $|\lambda_\tau|$ on ωT_{ADJ} is $(\omega T_{\text{ADJ}}) / [1 + (\omega T_{\text{ADJ}})^2]^{1/2}$, which varies

TABLE 2. Adjustment times and freshwater replacement times calculated for three realistic cases using the numerical model, with varying river flow. For each case, both high- and low-flow situations are considered. The analytical theory predicts, for exchange-dominated cases, that $T_{\text{ADJ}} = (1/2)T_0$, whereas these results have a range of $T_{\text{ADJ}} = (1/6-1)T_0$.

System	Q_R ($\text{m}^3 \text{s}^{-1}$)	T_{ADJ} (days)	$T_0 = 1/2(L_0/\bar{u}_0)$ (days)
San Francisco Bay	100	25	115
	1000	4	12
Delaware Bay	100	36	224
	1000	11	25
Hudson River	100	31	78
	1000	3	3

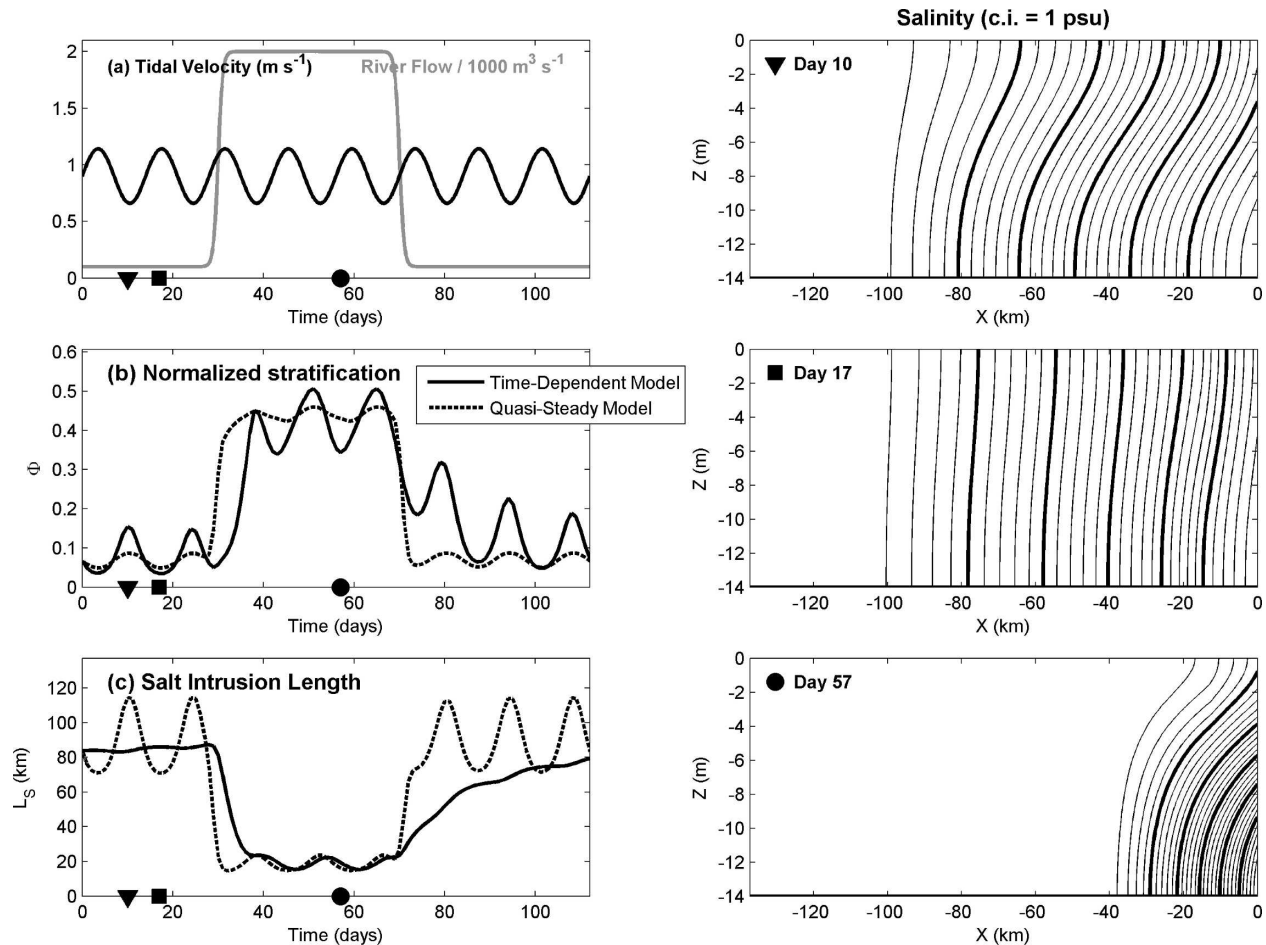


FIG. 5. Time-dependent numerical simulation of the Hudson River estuary. (a) The forcing variation, which consists of a spring–neap cycle of tidal amplitude and a switch from low river flow to high and back again. (b) The response of the model stratification with time, where the parameter Φ is the normalized stratification averaged over the length of the salt intrusion. (c) The length of the salt intrusion vs time. In (b) and (c), a quasi-steady model solution is also plotted to indicate how important unsteady effects might be. (right) Salinity sections at three times. These are from low-flow neap, low-flow spring, and high-flow periods. During low-flow periods, the stratification is relatively sensitive to the spring–neap cycle and the salt intrusion is not, in comparison with the quasi-steady solution. This result is because the salt intrusion does not have time to adjust.

between 0 and 1, and so one would expect greater Φ variation when λ is out of equilibrium.

The interplay among adjustment time, salt intrusion length, and stratification in a more realistic example may be illustrated using the numerical model. The Hudson River case is forced with changing river flow and a typical spring–neap variation of U_T (Fig. 5). This has the full mixing parameterizations derived in section 3. Also plotted is the quasi-steady solution, which is calculated by allowing the estuary to equilibrate with the instantaneous values of Q_R and U_T at each time step of the integration. For low-flow conditions, $\omega T_{\text{ADJ}} = 2\pi(31 \text{ days})/(14 \text{ days}) = 14$, implying that the sensitivity of L is reduced to 7% of its quasi-steady value. During high flow, on the other hand, it is only reduced to 60%. In the converse situation, the relative sensitivity of

stratification is greater during low flow. The adjustment time is also apparent in the lag of L relative to the steps in Q_R , with the step from high to low flow being slower (Kranenburg 1986). For this system, it is apparent that the quasi-steady solution may stray significantly from the time-dependent solution.

6. Summary and conclusions

Starting from the same classical equations used by Hansen and Rattray (1965), Chatwin (1976), and others, I have developed a model of tidally averaged, width-averaged estuarine circulation and salinity. The model improves on its predecessors by allowing variation of channel depth and width and allowing time-dependent forcing. I have also made an attempt to de-

velop plausible parameterizations of the effective eddy viscosity, diffusivity, and tidal stirring coefficients (K_M , K_S , and K_H), building on work by Geyer et al. (2000), MacCready (1999, 2004), Peters (1999), and Banas et al. (2004). An important step in these parameterizations is that they depend only on the channel geometry, the tidal current amplitude (U_T , a known forcing parameter), and the tidally averaged stratification (a state variable). By doing this, spring–neap variation in U_T can sensibly affect the mixing coefficients. Also, the mixing coefficients are no longer treated as fitting parameters, as was done in Hansen and Rattray (1965) (although I have certainly engaged in some fitting in choosing the unknown constants in the three mixing coefficients, as well as in choosing their functional forms!). The resulting model did a reasonable job of reproducing the curves for salt intrusion versus Q_R for the Hudson River estuary and north San Francisco Bay. It was less successful in the Delaware Bay, predicting a salt intrusion that is too long, especially during low flow.

The model appears to be able to work for systems ranging from well mixed to strongly stratified (see Fig. 5), but it cannot create a salt wedge. This is because the x momentum equation has been linearized and \bar{s}_x is assumed to be constant in z . The vertical structure functions (cubic and quintic profiles for velocity and salinity) rely on the assumptions that 1) channel geometry varies slowly along the channel, 2) \bar{s}_x is constant in z , and 3) the mixing coefficients are constant in z . As a consequence, the model is completely inappropriate for fjordlike systems such as the Puget Sound. A final important caveat about model limitations is that I have not addressed channel cross-sectional shape in any sensible way, and this has been suggested as an important consideration (Fischer 1972; Smith 1980).

The time-dependent model equations were linearized and scaled down to the point at which the evolution of the salt intrusion could be represented by a dimensionless, first-order, linear ODE with forcing and damping. This equation offers, it is hoped, a much clearer view of the system response characteristics than those given earlier by Kranenburg (1986) and MacCready (1999). An equation of the same form was used by Monismith et al. (2002) and Hetland and Geyer (2004). The contribution of this paper is to justify rigorously why an equation of this form is pertinent and to predict what its coefficients should be. Results that follow from this equation have, to some extent, appeared in the previous literature. In this paper, I am able to offer explanations for some of Kranenburg's (1986) adjustment time results and give theoretical support for Kranenburg's assertion that the adjustment time should

be the same for changes in both Q_R and U_T , despite the strongly different sensitivity to these forcing terms.

Last, the potential utility of the numerical model is demonstrated in section 5, in which it is used to simulate the Hudson River response to order-of-magnitude changes in Q_R superimposed on the spring–neap cycle of U_T . Although the model has significant limitations in comparison with the remarkable 3D simulations of Warner et al. (2005), it is fast to run (about 2 min for the simulation in Fig. 5) and is very easy to reconfigure.

Acknowledgments. This work was generously supported by NSF Grant OCE-0136760 and NOAA Grant NA04NOS4730156. I am indebted to Rocky Geyer, James Lerczak, Rob Hetland, Neil Banas, and Stephen Monismith for many discussions of these ideas.

REFERENCES

- Abood, K. A., 1974: Circulation in the Hudson River estuary. *Hudson River Colloquium*, O. A. Roels, Ed., Annals of the New York Academy of Sciences, Vol. 250, New York Academy of Sciences, 38–111.
- Banas, N. S., B. M. Hickey, P. MacCready, and J. A. Newton, 2004: Dynamics of Willapa Bay, Washington: A highly unsteady, partially mixed estuary. *J. Phys. Oceanogr.*, **34**, 2413–2427.
- Bowen, M. M., 2000: Mechanisms and variability of salt transport in partially-stratified estuaries. Ph.D. thesis, Massachusetts Institute of Technology/Woods Hole Oceanographic Institution, MIT/WHOI 00-04, 171 pp.
- Chatwin, P. C., 1976: Some remarks on the maintenance of the salinity distribution in estuaries. *Estuarine Coastal Mar. Sci.*, **4**, 555–566.
- Dyer, K. R., 1997: *Estuaries: A Physical Introduction*. 2d ed. John Wiley and Sons, 195 pp.
- Fischer, H. B., 1972: Mass transport mechanisms in partially stratified estuaries. *J. Fluid Mech.*, **53**, 671–687.
- Garvine, R. W., R. K. McCarthy, and K.-C. Wong, 1992: The axial salinity distribution in the Delaware estuary and its weak response to river discharge. *Estuarine Coastal Shelf Sci.*, **35**, 157–165.
- Geyer, W. R., J. H. Trowbridge, and M. M. Bowen, 2000: The dynamics of a partially mixed estuary. *J. Phys. Oceanogr.*, **30**, 2035–2048.
- Hansen, D. V., and M. Rattray, 1965: Gravitational circulation in straits and estuaries. *J. Mar. Res.*, **23**, 104–122.
- Hetland, R. D., and W. R. Geyer, 2004: An idealized study of the structure of long, partially mixed estuaries. *J. Phys. Oceanogr.*, **34**, 2677–2691.
- Kranenburg, C., 1986: A time scale for long-term salt intrusion in well-mixed estuaries. *J. Phys. Oceanogr.*, **16**, 1329–1331.
- Lewis, R. E., 1996: Relative contributions of interfacial and bed generated mixing to the estuarine energy balance. *Mixing in Estuaries and Coastal Seas*, C. Pattiaratchi, Ed., Coastal and Estuarine Studies, Vol. 50, Amer. Geophys. Union, 250–266.
- MacCready, P., 1999: Estuarine adjustment to changes in river flow and tidal mixing. *J. Phys. Oceanogr.*, **29**, 708–726.
- , 2004: Toward a unified theory of tidally-averaged estuarine salinity structure. *Estuaries*, **27**, 561–570.
- Monismith, S. G., W. Kimmerer, J. R. Burau, and M. T. Stacey,

- 2002: Structure and flow-induced variability of the subtidal salinity field in northern San Francisco Bay. *J. Phys. Oceanogr.*, **32**, 3003–3018.
- Munk, W. H., and F. R. Anderson, 1948: Notes on a theory of the thermocline. *J. Mar. Res.*, **7**, 276–295.
- Park, K., and A. Y. Kuo, 1996: Effect of variation in vertical mixing on residual circulation on narrow, weakly nonlinear estuaries. *Buoyancy Effects on Coastal and Estuarine Dynamics*, D. G. Aubrey and C. T. Friedrichs, Eds., Amer. Geophys. Union, 301–317.
- Peters, H., 1999: Spatial and temporal variability of turbulent mixing in an estuary. *J. Mar. Res.*, **57**, 805–845.
- Press, W. H., S. A. Teukolsky, W. T. Vetterling, and B. P. Flannery, 1992: *Numerical Recipes in C: The Art of Scientific Computing*. 2d ed. Cambridge University Press, 994 pp.
- Smith, R., 1980: Buoyancy effects upon longitudinal dispersion in wide well-mixed estuaries. *Philos. Trans. Roy. Soc. London*, **296A**, 467–496.
- Stommel, H., and H. G. Farmer, 1952: On the nature of estuarine circulation, Part I. Woods Hole Oceanographic Institute Tech. Rep. 52-88, 131 pp.
- Uncles, R. J., and J. A. Stephens, 1990: The structure of vertical current profiles in a macrotidal, partially-mixed estuary. *Estuaries*, **13**, 349–361.
- Warner, J. C., W. R. Geyer, and J. A. Lerczak, 2005: Numerical modeling of an estuary: A comprehensive skill assessment. *J. Geophys. Res.*, **110**, C05001, doi:10.1029/2004JC002691.